

# Power-Efficient Wireless Neural Stimulating System Design for Implantable Medical Devices

Hyung-Min Lee<sup>1,2</sup> and Maysam Ghovanloo<sup>1</sup>

<sup>1</sup>School of Electrical and Computer Engineering, Georgia Institute of Technology / Atlanta, GA 30308, USA  
mgh@gatech.edu

<sup>2</sup>Department of Electrical Engineering and Computer Science, Massachusetts Institute of Technology / Cambridge, MA 02139, USA hyungmin@mit.edu

\* Corresponding Author: Maysam Ghovanloo

Received May 13, 2015; Accepted June 15, 2015; Published June 30, 2015

\* Regular Paper

**Abstract:** Neural stimulating implantable medical devices (IMDs) have been widely used to treat neurological diseases or interface with sensory feedback for amputees or patients suffering from severe paralysis. More recent IMDs, such as retinal implants or brain-computer interfaces, demand higher performance to enable sophisticated therapies, while consuming power at higher orders of magnitude to handle more functions on a larger scale at higher rates, which limits the ability to supply the IMDs with primary batteries. Inductive power transmission across the skin is a viable solution to power up an IMD, while it demands high power efficiencies at every power delivery stage for safe and effective stimulation without increasing the surrounding tissue's temperature. This paper reviews various wireless neural stimulating systems and their power management techniques to maximize IMD power efficiency. We also explore both wireless electrical and optical stimulation mechanisms and their power requirements in implantable neural interface applications.

**Keywords:** Neural stimulation, Wireless power transfer, Implantable medical devices, Optogenetics

## 1. Introduction

Implantable medical devices (IMDs) with stimulating functions have proven to be effective therapies to alleviate neurological diseases or substitute sensory modalities lost due to disease or injury [1, 2]. These implantable stimulators are capable of injecting a designated amount of charge into the surrounding tissue by providing a precise amount of output current or output voltage between two or more electrodes for a predefined period. Deep brain stimulation (DBS) is one of the most effective examples of such therapies to treat several diseases, such as Parkinson's disease, tremor, and dystonia [3, 4]. However, today's DBS devices suffer from having large primary batteries implanted in the chest, where there is more space available, instead of the brain. Therefore, they need subcutaneous interconnects to pass across the neck to reach the electrodes implanted deep in the brain. This increases the complexity of implantation surgery and the risks of mechanical interconnect failure due to head motion [5]. Moreover, batteries need to be replaced every two to five

years through additional surgery. As a promising solution, a head-mounted DBS can reduce the risk and hardship imposed by a chest-implanted primary battery and long interconnects across the neck, replacing them with a pair of coils and transcutaneous inductive power transfer from a behind-the-ear (BTE) rechargeable energy source, similar to cochlear implants or hearing aids [6-8].

Fig. 1 shows a conceptual configuration of a head-mounted inductively powered DBS system as an alternative to the conventional chest-implanted battery-powered DBS [9]. An external processing unit, which includes a rechargeable battery, provides transcutaneous power and data through a pair of loosely-coupled coils. The induced AC input across the implanted coil supplies the rest of the DBS implant through an efficient power-management unit. The DBS system generates stimulus pulses, which are delivered to the stimulation sites through individual leads that are significantly shorter than those from the chest area. Therefore, the head-mounted inductively-powered system is less invasive and potentially more suitable for high-density DBS [10]. Like

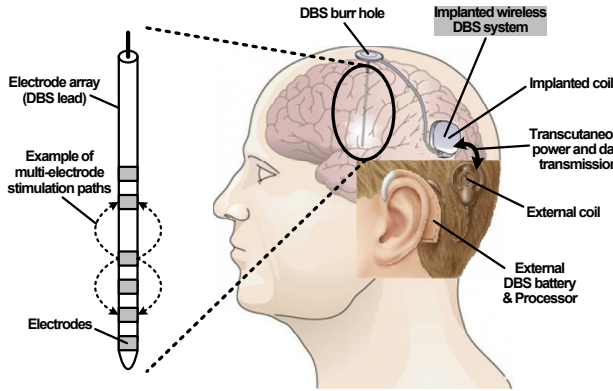


**Fig. 1. Conceptual configuration of a head-mounted inductively powered DBS system in which power and data are transferred through an inductive link [9].**

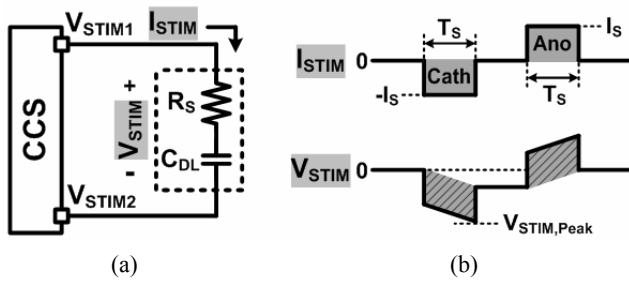


**Fig. 2. (a) A current-controlled stimulation (CCS) system stimulating a simplified electrode and tissue model, (b) the resulting stimulation current and voltage waveforms.**

other wirelessly powered IMDs, high power efficiency is paramount in reducing the risk of tissue damage from overheating as well as extending the range of a wireless power transmission link and external battery life [11, 12].

The next step is adopting efficient stimulating schemes and power management techniques to further improve DBS efficiency. Voltage-controlled stimulation (VCS) enables power-efficient stimulation. However, balancing the stimulation charge is quite complicated in VCS because the electrode impedance can vary over time and position [4, 13]. On the other hand, current-controlled stimulation (CCS) has been widely used because of its precise charge control and safe operation by using current sources [14]. Fig. 2 shows the biphasic (cathodic-anodic) stimulation current and voltage waveforms when the CCS system drives a simplified pair of electrodes and tissue model, a series  $R_S$  and  $C_{DL}$ , which represent tissue spreading resistance and double-layer capacitance, respectively. The CCS system is capable of injecting charge-balanced biphasic stimuli ( $Q = I \times T$ ) by adjusting stimulation current level,  $I_S$ , and duration,  $T_S$ . However, the CCS system suffers from low power efficiency because of the dropout voltage across its current sources, particularly when the stimulation voltage,  $V_{STIM}$ , is much smaller than the CCS supply voltage. Moreover, inductively powered stimulating systems with any stimulation mechanism need a rectifier and a regulator to convert the radio frequency (RF) input to the DC supply voltage, which results in

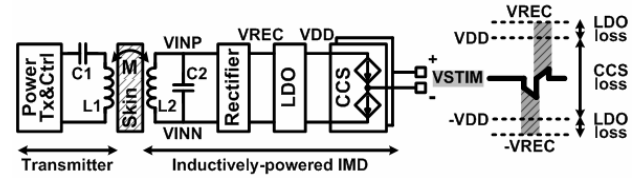


**Fig. 3. Block diagram of a conventional inductively powered current-controlled stimulation (CCS) system with emphasis on key blocks for power transfer.**

additional power losses, further decreasing the overall stimulation efficiency.

In this paper, we review various inductively powered neural stimulating systems and their circuit techniques to increase IMD power efficiency while ensuring safe stimulation. We also explore the recently introduced optogenetic stimulation, the optical stimulation of neural circuits [15], and discuss the power limitations and potential solutions for implantable wireless optogenetic stimulators.

## 2. Inductively Powered Stimulating IMDs

Fig. 3 shows a block diagram of a conventional inductively powered CCS system with emphasis on key blocks for power transfer to the stimulator outputs. The wireless transcutaneous power is commonly delivered from an RF power transmitter (Tx) to an IMD (Rx) through an inductive link and power management units. The power Tx, which is supplied by an external energy source, drives a primary coil,  $L_1$ , at the power carrier frequency,  $f_p$ . An AC signal is induced across a secondary coil,  $L_2$ , because of the coils' electromagnetic flux coupling. The Rx inductive-capacitive resonance circuit,  $L_2C_2$ -tank, which is tuned at  $f_p$ , boosts the AC voltages,  $V_{INP}$  and  $V_{INN}$ , across the  $L_2C_2$ -tank. Then, the IMD utilizes a rectifier to convert the AC input to a DC output,  $V_{REC}$ , followed by a low-dropout (LDO) regulator to generate a fixed supply voltage,  $V_{DD}$ , for the rest of the system. However, this simple structure wastes a large portion of the input power across the rectifier, LDO, and current sources in the CCS method. The LDO loss increases when  $V_{REC}$ , which depends on the AC input amplitude, increases. The CCS loss also increases as the peak  $V_{STIM}$ , *i.e.* the maximum voltage across the electrodes and tissue model (see Fig. 2), becomes smaller.

Recently, several circuit techniques have been proposed to improve overall power efficiency in wireless neural stimulating IMDs. Fig. 4 compares various inductively powered stimulating structures, while all structures were assumed to provide bipolar and biphasic stimulation pulses through a similar pair of electrodes. We have also assumed that the inductive link can maintain its peak efficiency against reflected impedance variations as the stimulator loading changes using a multi-coil inductive link or adaptive resonant load transformation [16-18]. Here, we focus on power efficiency of the stimulating IMD, which can be defined as the ratio of the RF input power

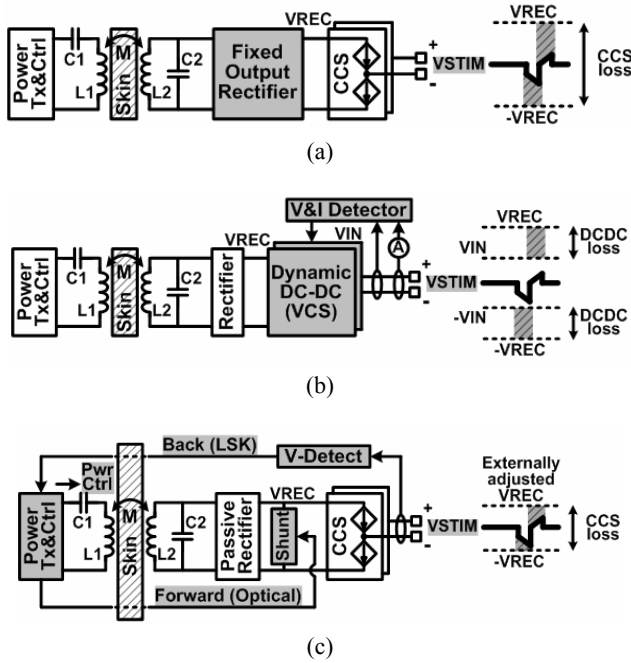


**Fig. 4. Various inductively powered stimulating IMD structures with (a) a fixed output rectifier [19][19], (b) a dynamic DC-DC converter [20], (c) an external closed-loop supply control [21, 22].**

from the secondary coil to the stimulator output power delivered to the tissue.

In Fig. 4(a), a fixed output rectifier was proposed to generate a predefined constant  $V_{REC}$  without an LDO [19]. Eliminating the LDO reduced the loss, but the CCS loss was still dominant during stimulation, especially when  $V_{STIM} \ll V_{REC}$ . It also needs an auxiliary rectifier to supply the fixed output rectifier. A stimulator from Arfin and Sarpeshkar [20] utilized a dynamic supply voltage,  $V_{IN}$ , from a DC-DC converter, as shown in Fig. 4(b). It achieved high efficiency from VCS as well as coarse current controllability. However, it still required constant DC input,  $V_{REC}$ , from the rectifier, leading to a loss added to that of the DC-DC converter ( $\eta_{DCDC} = 55 \sim 94\%$ ).

In Fig. 4(c), the inductive power delivered to the stimulator was adjusted through an external closed loop, changing  $V_{REC}$  to be near the peak voltage of  $V_{STIM}$ , leading to small power loss across the current sources in CCS [21, 22]. However, the external control loop via load-shift-keying (LSK), which adjusts the inductive coupling by shorting the  $L_2C_2$ -tank for a short time ( $< 1 \mu s$ ), is prone to interference and can be interrupted in loosely coupled inductive links, while increasing the system design complexity. The passive rectifier also induces a larger AC-DC loss than the active rectifier, which further decreases the overall power efficiency [23]. It should be pointed out that the methods used in these inductively powered stimulating structures may be used together to improve overall power efficiency.

Further improving the stimulation power efficiency of the inductively powered stimulators under limited received power through the inductive link is highly desired. Moreover, the shape of the stimulus waveform can also be

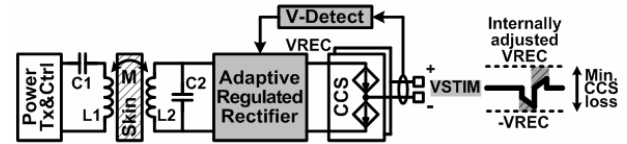


**Fig. 5. Conceptual block diagram of the inductively powered wireless stimulating system with adaptive supply control [9].**

considered as a factor on the biological side to further improve the stimulus efficacy in addition to the stimulator efficiency on the IMD side [24, 25].

### 3. Wireless Stimulating System with Adaptive Supply Control

In order to achieve both safe and power-efficient stimulation, a wireless neural stimulating system with adaptive supply control was proposed [9]. In this system, the stimulator supply voltage is automatically adjusted near the required peak stimulation voltage by detecting the site potential and forming a closed control loop through an efficient adaptive regulated rectifier. This mechanism minimizes power losses across current sources in the CCS as well as the adaptive regulated rectifier, resulting in higher IMD power efficiency for neural stimulation. The stimulation system also adopts active charge balancing by sharing the closed-loop path of the adaptive supply control to inject small current pulses in the tissue to keep the residual charges within a safe limit [4, 26].

Fig. 5 shows a conceptual block diagram of the inductively powered wireless stimulating system with adaptive supply control. The adaptive regulated rectifier with active switching is capable of generating a multilevel DC voltage,  $V_{REC}$ , directly from the AC input voltage across  $L_2$  through an internal closed-loop supply control mechanism. Therefore,  $V_{REC}$ , which directly supplies the CCS without an LDO, is adaptively adjusted close to the peak of  $V_{STIM}$ , resulting in minimum loss while benefiting from the safety feature of the CCS. Moreover, the adaptive regulated rectifier achieves high AC-DC power conversion efficiency (PCE) by adopting phase control feedback and active synchronous rectification to improve the overall power efficiency of the inductively powered stimulator.

In order for the adaptive regulated rectifier to generate the desired multilevel  $V_{REC}$  without using the regulator, the rectifier turn-on time needs to be adjusted to limit the forward current, while achieving high PCE. Fig. 6 shows the simplified voltage waveforms of the rectifier depending on the turn-on time. Conventional rectifiers aim to generate the maximum  $V_{REC}$  from  $V_{IN(AC)}$  at high PCE. Therefore, they turn on as long as  $V_{IN(AC)} > V_{REC}$ , as shown in Fig. 6(a). Consequently,  $V_{REC}$  becomes dependent on the  $V_{IN(AC)}$  amplitude, and it is not internally adjustable. To internally adjust  $V_{REC}$ , the adaptive regulated rectifier controls the turn-on phase, as shown in Fig. 6(b). In this method, the rectifier turns on when  $V_{IN(AC)} > V_{REC}$ , similar to the conventional rectifiers. However, its turn-off timing

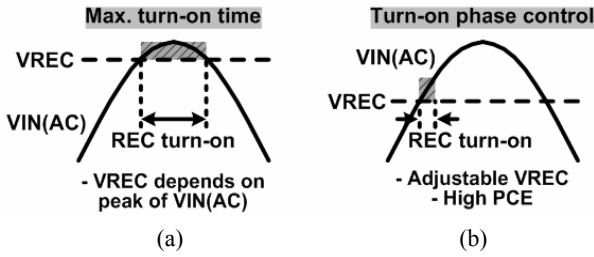


Fig. 6. Simplified voltage waveforms of (a) the conventional rectifier, (b) the adaptive regulated rectifier with turn-on phase control.

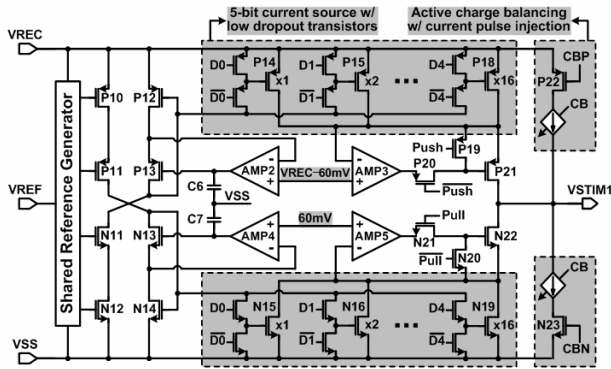


Fig. 7. Schematic diagram of the current-controlled stimulator with low dropout 5-bit current sources and active charge balancing [9].

is controlled to limit the forward current. Therefore,  $V_{REC}$  is adjustable depending on the rectifier turn-on phase, while the small dropout voltage between  $V_{IN}(AC)$  and  $V_{REC}$  during the on period provides high PCE.

Fig. 7 shows a schematic diagram of a current-controlled stimulator [9]. The current stimulator is equipped with a pair of low-dropout 5-bit current sources, while being supplied from the adaptive  $V_{REC}$ , as shown in Fig. 5. Feedback loops using AMP<sub>2-5</sub> set the drain-source voltages of P<sub>14</sub> ~ P<sub>18</sub> and N<sub>15</sub> ~ N<sub>19</sub> at  $\sim 60\text{ mV}$  in the triode region. Therefore, the voltage headroom of the output stage,  $V_{Head}$ , can drop down to  $V_{DS,sat} + 60\text{ mV}$ , which is smaller than  $2V_{DS,sat}$  of a typical cascode output stage. The two current stimulators source and sink at the same time, providing a bipolar stimulation compliance voltage of  $V_{REC} - 2V_{Head}$ . The 5-bit current sources with binary-weighted transistors are placed at the output stage directly to reduce the stimulator power loss, compared to using current mirrors after a 5-bit current DAC in [21]. In addition, the active charge balancing circuits push or pull additional small current pulses to the load after stimulation until the residual site voltage settles within a  $\pm 50\text{ mV}$  safety window [26]. This scheme is capable of estimating the required charge-balancing period.

Fig. 8 compares the overall power efficiency vs.  $I_{STIM}$  between using an adaptive supply,  $V_{REC}$ , and a fixed supply,  $V_{DD}$ , when stimulating the series RC model with  $R_S = 2\text{ k}\Omega$  and  $C_{DL} = 500\text{ nF}$  for  $T_S = 400\text{ }\mu\text{s}$ . The adaptive supply control automatically adjusts  $V_{REC}$  between 2.5 V and 4.6 V with 0.3 V increments, while the fixed supply sets  $V_{DD} =$

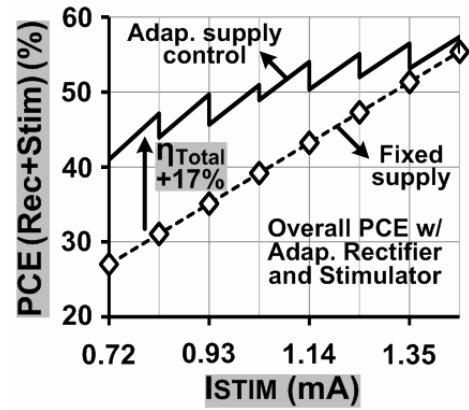


Fig. 8. Overall power efficiencies of stimulating IMDs with adaptive supply control and fixed supply [9].

4.6 V. The adaptive supply control leads to higher overall power efficiency (41 ~ 58%), which includes efficiencies of the adaptive regulated rectifier and the current stimulator, compared with using the fixed supply (27 ~ 55%).

#### 4. Wireless Switched-Capacitor Stimulation (SCS) System

Switched-capacitor stimulation (SCS), proposed in [27], takes advantage of both high efficiency of VCS and safety of CCS by using capacitor banks to transfer quantized amounts of charge to the tissue. Vidal and Ghovanloo [13] only presented a discrete version of the SCS with no on-chip integration. The stimulating system of Kelly and Wyatt [28] also adopts the SCS mechanism to construct pseudo-rectangular stimuli, using multiple decaying exponential pulses, but it suffers from poor voltage-based capacitor charging efficiency, which is always less than 50%.

Recently, an integrated wireless SCS system was proposed [29], which has inductive capacitor charging and charge-based stimulation capabilities for energy-efficient stimulation. Fig. 9 shows the conceptual block diagram of the inductive power flow from the external energy source to the tissue in the SCS systems as well as the resulting stimulus waveform. The streamlined inductively powered SCS efficiently charges the storage capacitors directly from the inductive link and delivers the quantized stored charge to the electrode/tissue, modeled by a series RC, improving stimulator efficiency. In addition, the SCS system is capable of generating a decaying exponential stimulus by dumping the capacitor charge in the tissue without wasting additional power. This decaying exponential stimulus can be equally, if not more, effective in activating a larger target tissue area, compared to the conventional rectangular stimuli, while consuming the same amount of energy, thus improving both stimulus efficacy and safety [24, 25].

Fig. 10 shows a simplified block diagram of the SCS system that can efficiently charge a positive/negative capacitor bank,  $C_P$  and  $C_N$ , directly from AC input voltage



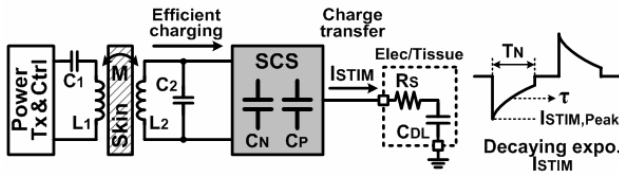


Fig. 9. Conceptual diagram of the wireless switched-capacitor stimulating (SCS) system [29].

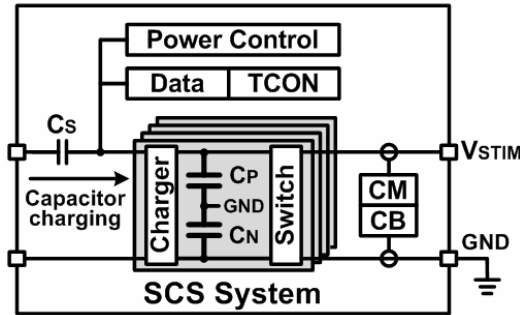


Fig. 10. Simplified block diagram of the SCS system with a focus on wireless capacitor charging and charge transfer to the tissue [29].

through a series capacitor,  $C_s$ , and an inductive charger, to improve capacitor charging efficiency. For efficient stimulation, the capacitor bank stores the energy being wirelessly delivered across the skin from the external battery and then transfers quantized amounts of the stored charge to the tissue. The charge stored in the capacitors is delivered to the load (*i.e.* two electrodes and the tissue in between) in a quantized fashion ( $Q = C \times V$ ) through low-resistance switches, which minimize the power losses, while creating exponentially decaying pulses. This SCS mechanism not only improves overall IMD power efficiency to ensure highly efficient charge-based stimulation, but also creates a buffer between the inductive link and the highly variable load without using any rectifiers and regulators.

For biphasic stimulation, the storage capacitor pairs are

alternately connected to the electrodes, injecting negative and positive charges into the tissue to evoke neural activity. A charge monitoring (CM) circuit measures the amount of injected charge and dynamically changes the pulse width of the subsequent stimulus to neutralize the residual charge in the tissue. Discharged capacitor pairs are continuously recharged to their target voltages, while a secondary charge balancing (CB) circuit prevents residual charge accumulation by shorting electrodes to ground for a predefined period following stimulation.

Table 1 benchmarks the state-of-the-art wireless neural stimulating systems with emphasis on their overall power efficiencies. The inductively powered stimulating systems, which utilize CCS or VCS, require the rectifier, regulator, current driver, and even DC-DC converter to generate rectangular stimuli, while power losses at each stage result in poor overall stimulation efficiencies. On the other hand, the SCS systems can generate decaying exponential pulses, which can be more effective in activating neural tissue than rectangular pulses while consuming the same amount of stimulus energy. The overall SCS power efficiency mainly depends on its capacitor charging efficiency, which needs to be optimally designed. It should be noted that the overall stimulation efficiency may also vary depending on electrode/tissue impedance as well as stimulus pulse width in various applications.

### 5. Wireless Optogenetic System

Optical stimulation of genetically modified neurons, known as optogenetics, has become an effective way to selectively generate neural activity using various light-delivery schemes. Optogenetics enables fast, spatially controlled, and minimally invasive modulation of target cells compared to electrical stimulation [31]. In addition, the optical stimulation is capable of eliminating electrical artifacts, while enabling extended lifetime by hermetic sealing of the light sources [32].

There are several light-delivery schemes for optical stimulation, such as a laser-coupled optical fiber and a single light-emitting diode (LED). However, they suffer

Table 1. Inductively powered stimulating system benchmarking.

Publication	2010 [30]	2012 [20]	2013 [9]	2011 [28]	2015 [29]	
Technology	0.18 $\mu\text{m}$ HV	0.35 $\mu\text{m}$	0.5 $\mu\text{m}$	1.5 $\mu\text{m}$	0.35 $\mu\text{m}$	
Stimulator structure	CCS	VCS + CCS	Adaptive CCS	SCS	SCS	
Supply voltage (V)	$\pm 12$	3.3	2.5 ~ 4.6	$\pm 1.75$ (Cap)	$\pm 2$ (Cap)	
Max. stimulator power efficiency (%)	Rect. + Reg.	85.6	80*	87	-	-
	DC-DC	-	74**	-	-	-
	Current drv.	41.6	-	68	-	-
	Charger+Sw	-	-	-	40***	80.4
	Total	35.6	59**	59	40	80.4
Current stimulus shape	Rectangular	Rectangular	Rectangular	Decaying expo.	Decaying expo.	
Injected $I_{STIM}$ (mA)	0.5	0.45	1.45	0.4 (peak)	4 (peak)	
Series RC model	10k $\Omega$ + 100nF	1k $\Omega$ + 0.93 $\mu\text{F}$	2k $\Omega$ + 0.5 $\mu\text{F}$	1.15k $\Omega$ + 1 $\mu\text{F}$	0.5k $\Omega$ + 1 $\mu\text{F}$	

\* Assuming a rectifier is needed, \*\* averaged, \*\*\* including power consumption of the other blocks.

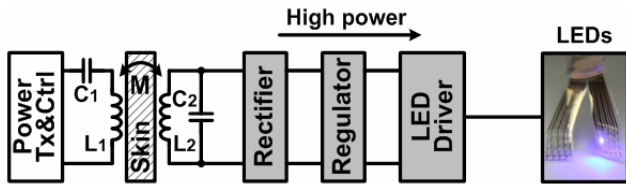


Fig. 11. Conceptual diagram of the conventional wireless optogenetic system with an LED driver [34].

from poor spatial resolution and tethering effects through wires and optical fibers. Recently, a multichannel 3-D optrode array, which integrates micro-LEDs with micro-needle waveguides, was proposed to minimize light scattering in the tissue and achieve high spatial resolution for long-term implantable optogenetics [33].

However, LEDs typically require high instantaneous power to emit sufficient light for optical neural stimulation, which can be a significant limiting factor in conventional IMDs [34]. Fig. 11 shows a conceptual diagram of the conventional inductively powered optogenetic system, which requires the rectifier and the regulator to convert AC input voltage to DC output voltage for supplying the LED driver. Power losses in these stages result in poor overall power efficiency from  $L_2$  to the LEDs. In addition, the high instantaneous power that flows to the LEDs leads to large load variation, which affects impedance matching with the inductive link. This can significantly increase the required inductive power level and create a safety issue by increasing the temperature while degrading the inductive link's power efficiency, due to impedance mismatch, and the supply voltage for the rest of the IMD.

To address these limitations, the SCS mechanism is utilized for power-efficient implantable optogenetics, as shown in Fig. 12(a) [35]. The SCS-based optogenetic system can efficiently charge an array of storage capacitors directly from the inductive link and periodically discharge them into the micro-LEDs, providing high instantaneous current without burdening the inductive link and system supply voltage. The efficient wireless capacitor charger also improves the optical stimulation power efficiency. After charging, a storage capacitor pair,  $C_P$  and  $C_N$ , can be connected in series to provide higher pulse-based LED driving voltage,  $V_{LED}$ , as shown in Fig. 12(b).

## 6. Conclusion

Wireless neural stimulating systems require high stimulation power efficiency to perform effective therapies through multiple sites, without raising the surrounding tissue temperature, and to operate with their limited available transcutaneous power. Various circuit and system-level techniques can be utilized in stimulating IMDs to efficiently generate stimulus pulses from the RF input power and precisely deliver them to the tissue. Power-efficient wireless stimulating systems can activate the target tissue with a minimum amount of energy from the inductive link, providing multiple advantages, such as extended-range wireless power transfer, less volume or

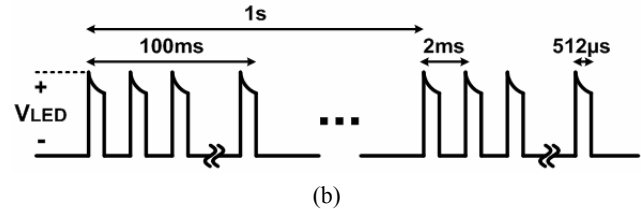
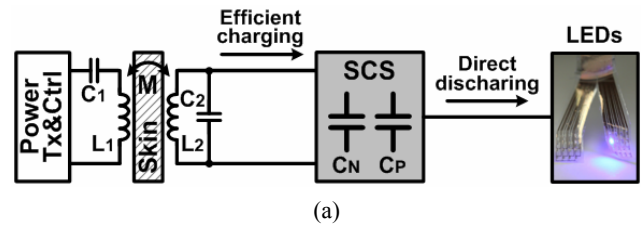


Fig. 12. (a) Conceptual diagram of the SCS-based wireless optogenetic system, (b) its pulse-based output voltage to drive LEDs [35].

longer lifetime of the external power Tx battery, a wide range of stimulus energy levels, efficacious and safe stimulation, and a lower risk of tissue damage from overheating.

## Acknowledgement

This work was supported in part by National Institute of Biomedical Imaging and Bioengineering grant 1R21EB018561 and the National Science Foundation under awards IIP-1439426, ECCS-1407880, and ECCS-1408318.

## References

- [1] L. D. Cruz, et al, "The Argus II epiretinal prosthesis system allows letter and word reading and long-term function in patients with profound vision loss," *Br. J. Ophthalmol.* Feb. 2013. [Article \(CrossRef Link\)](#)
- [2] A. V. Nurmikko, et al, "Listening to brain microcircuits for interfacing with external world-progress in wireless implantable microelectronic neuro-engineering devices," *Proc. IEEE*, vol. 98, pp. 375-388, Mar. 2010. [Article \(CrossRef Link\)](#)
- [3] A.M. Kuncel and W.M. Grill, "Selection of stimulus parameters for deep brain stimulation," *Clin. Neurophysiol.*, vol. 115, iss. 11, pp. 2431-2441, Nov. 2004. [Article \(CrossRef Link\)](#)
- [4] D.R. Merrill, M. Bikson, and J.G.R. Jefferys, "Electrical stimulation of excitable tissue: design of efficacious and safe protocols," *J. Neuroscience Methods*, vol. 141, pp. 171-198, Feb. 2005. [Article \(CrossRef Link\)](#)
- [5] S.K. Moore, "Psychiatry's shocking new tools," *IEEE Spectrum*, vol. 43, issue 3, pp. 24-31, Mar. 2006. [Article \(CrossRef Link\)](#)
- [6] B. S. Wilson and M. F. Dorman, "Cochlear implants: A remarkable past and a brilliant future," *Hearing*

- Res., vol. 242, no. 1-2, pp. 3-21, Aug. 2008. [Article \(CrossRef Link\)](#)
- [7] M. Ghovanloo and K. Najafi, "A wireless implantable multichannel microstimulating system-on-a-chip with modular architecture," *IEEE Trans. Neural Sys. Rehab. Eng.*, vol. 15, no. 3, pp. 449-457, Sept. 2007. [Article \(CrossRef Link\)](#)
- [8] M. Rasouli and L. S. Phee, "Energy sources and their development for application in medical devices," *Expert review of Medical Devices*, vol. 7, no. 5, pp. 693-709, 2010. [Article \(CrossRef Link\)](#)
- [9] H.-M. Lee, H. Park, and M. Ghovanloo, "A power-efficient wireless system with adaptive supply control for deep brain stimulation," *IEEE J. Solid-State Circuits*, vol. 48, no. 9, pp. 2203-2216, Sep. 2013. [Article \(CrossRef Link\)](#)
- [10] H.C.F. Martens, E. Toader, M.M.J. Decre, D.J. Anderson, R. Vetter, D.R. Kipke, K.B. Baker, M.D. Johnson, and J.L. Vitek, "Spatial steering of deep brain stimulation volumes using a novel lead design," *Clin. Neurophysiol.*, vol. 122, iss. 3, pp. 558-566, Mar. 2011. [Article \(CrossRef Link\)](#)
- [11] G. Lazzi, "Thermal effects of bioimplants," *IEEE Eng. Med. Biol. Mag.*, vol. 24, no. 5, pp.75 -81, Sep. 2005. [Article \(CrossRef Link\)](#)
- [12] H.-M. Lee and M. Ghovanloo, "A high frequency active voltage doubler in standard CMOS using offset-controlled comparators for inductive power transmission," *IEEE Trans. Biomed. Circuits Syst.*, vol. 7, no. 3, pp. 213-224, Jun. 2013. [Article \(CrossRef Link\)](#)
- [13] J. Vidal and M. Ghovanloo, "Toward a switched-capacitor based stimulator for efficient deep-brain stimulation," in *Proc. IEEE Eng. in Med. and Biol. Conf. (EMBC)*, pp. 2927-2930, Sept. 2010. [Article \(CrossRef Link\)](#)
- [14] J. Simpson and M. Ghovanloo, "An experimental study of voltage, current, and charge controlled stimulation front-end circuitry," in *Proc. IEEE Intl. Symp. on Cir. and Sys. (ISCAS)*, pp. 325-328, May 2007. [Article \(CrossRef Link\)](#)
- [15] E. S. Boyden, F. Zhang, E. Bamberg, G. Nagel, and K. Deisseroth, "Millisecond-timescale, genetically targeted optical control of neural activity," *Nat. Neurosci.*, vol. 8, no. 9, pp. 1263-1268, Sep. 2005. [Article \(CrossRef Link\)](#)
- [16] M. Kiani, U. Jow, and M. Ghovanloo, "Design and optimization of a 3-coil inductive link for efficient wireless power transmission," *IEEE Trans. Biomed. Circuits Syst.*, vol. 5, no. 6, pp. 579-591, Dec. 2011. [Article \(CrossRef Link\)](#)
- [17] R. Xue, K. Cheng, and M. Je, "High-efficiency wireless power transfer for biomedical implants by optimal resonant load transformation," *IEEE Trans. Circuits Syst. I*, vol. 60, no. 4, pp. 867-874, Apr. 2013. [Article \(CrossRef Link\)](#)
- [18] M. Kiani, B. Lee, P. Yeon, and M. Ghovanloo, "A power-management ASIC with Q-modulation capability for efficient inductive power transmission," in *IEEE Int. Solid-State Circuits Conf. (ISSCC) Dig. Tech. Papers*, Feb. 2015, pp. 226-227. [Article \(CrossRef Link\)](#)
- [19] K. F. E. Lee, "A timing controlled AC-DC converter for biomedical implants," in *IEEE Int. Solid-State Circuits Conf. (ISSCC) Dig. Tech. Papers*, Feb. 2010, pp. 128-129. [Article \(CrossRef Link\)](#)
- [20] S. Arfin and R. Sarpeshkar, "An energy-efficient, adiabatic electrode stimulator with inductive energy recycling and feedback current regulation," *IEEE Trans. Biomed. Circuits Syst.*, vol. 6, no. 1, pp. 1-14, Feb. 2012. [Article \(CrossRef Link\)](#)
- [21] E. Noorsal, K. Sooksood, H. Xu, R. Hornig, J. Becker, and M. Ortmanns, "A neural stimulator frontend with high-voltage compliance and programmable pulse shape for epiretinal implants," *IEEE J. Solid-State Circuits*, vol. 47, no. 1, pp. 244-256, Jan. 2012. [Article \(CrossRef Link\)](#)
- [22] H. Xu, E. Noorsal, K. Sooksood, J. Becker, and M. Ortmanns, "A multichannel neurostimulator with transcutaneous closed-loop power control and self-adaptive supply," in *IEEE Eur. Solid-State Circuits Conf. (ESSCIRC)*, Sept. 2012. [Article \(CrossRef Link\)](#)
- [23] H.-M. Lee and M. Ghovanloo, "An integrated power-efficient active rectifier with offset-controlled high speed comparators for inductively-powered applications," *IEEE Trans. Circuits Syst. I*, vol. 58, no. 8, pp. 1749-1760, Aug. 2011. [Article \(CrossRef Link\)](#)
- [24] A. Wongsarnpigoon, J. P. Woock, and W. M. Grill, "Efficiency analysis of waveform shape for electrical excitation of nerve fibers," *IEEE Trans. Neural Syst. Rehab. Eng.*, vol. 18, no. 3, pp. 319-328, June 2010. [Article \(CrossRef Link\)](#)
- [25] A. Wongsarnpigoon and W. M. Grill, "Energy-efficient waveform shapes for neural stimulation revealed with a genetic algorithm," *J. Neural Eng.*, vol. 7, no. 4, June 2010. [Article \(CrossRef Link\)](#)
- [26] K. Sooksood, T. Stieglitz, and M. Ortmanns, "An active approach for charge balancing in functional electrical stimulation," *IEEE Trans. Biomed. Circuits Syst.*, vol. 4, no. 3, pp. 162-170, Jun. 2010. [Article \(CrossRef Link\)](#)
- [27] M. Ghovanloo, "Switched-capacitor based implantable low-power wireless microstimulating systems," in *Proc. IEEE Intl. Symp. on Cir. and Sys. (ISCAS)*, pp. 2197-2200, May 2006. [Article \(CrossRef Link\)](#)
- [28] S. Kelly and J. Wyatt, "A power-efficient neural tissue stimulator with energy recovery," *IEEE Trans. Biomed. Circuits Syst.*, vol. 5, no. 1, pp. 20-29, Feb. 2011. [Article \(CrossRef Link\)](#)
- [29] H.-M. Lee, K. Y. Kwon, W. Li, and M. Ghovanloo, "A power-efficient switched-capacitor stimulating system for electrical/optical deep brain stimulation," *IEEE J. Solid-State Circuits*, vol. 50, no. 1, pp. 360-374, Jan. 2015. [Article \(CrossRef Link\)](#)
- [30] K. Chen, Z. Yang, L. Hoang, J. Weiland, M. Humayun, and W. Liu, "An integrated 256-channel epiretinal prosthesis," *IEEE J. Solid-State Circuits*, vol. 45, no. 9, pp. 1946-1956, Sep. 2010. [Article \(CrossRef Link\)](#)

- [31] F. Zhang, A. Aravanis, A. Adamantidis, L. de Lecea, and K. Deisseroth, "Circuit-breakers: optical technologies for probing neural signals and systems," *Nat. Rev. Neurosci.*, vol. 8, no. 8, pp. 577–581, Aug. 2007. [Article \(CrossRef Link\)](#)
- [32] V. Gilja, C. A. Chestek, I. Diester, J. M. Henderson, K. Deisseroth, and K. V. Shenoy, "Challenges and opportunities for next-generation intracortically based neural prostheses," *IEEE Trans. Biomed. Eng.*, vol. 58, no. 7, pp. 1891–1899, Jul. 2011. [Article \(CrossRef Link\)](#)
- [33] K. Kwon, H.-M. Lee, M. Ghovanloo, A. Weber, and W. Li, "A wireless slanted optrode array with integrated micro LEDs for optogenetics," in *Prof. IEEE Int. Conf. Micro Electro Mech. Systems (MEMS)*, Jan. 2014. [Article \(CrossRef Link\)](#)
- [34] C. T. Wentz, J. G. Bernstein, P. Monahan, A. Guerra, A. Rodriguez, and E. S. Boyden, "A wirelessly powered and controlled device for optical neural control of freely-behaving animals," *J. Neural Eng.*, vol. 8, no. 4, Jun. 2011. [Article \(CrossRef Link\)](#)
- [35] H.-M. Lee, K.-Y. Kwon, W. Li, and M. Ghovanloo, "A wireless implantable switched-capacitor based optogenetic stimulating system," *IEEE Eng. Med. Biol. Conf. (EMBC)*, pp. 878–881, Aug. 2014. [Article \(CrossRef Link\)](#)



**Hyung-Min Lee** received a BSc in electrical engineering (*summa cum laude*) from Korea University, Seoul, Korea, in 2006, an MSc in electrical engineering from the Korea Advanced Institute of Science and Technology (KAIST), Daejeon, Korea, in 2008, and a PhD in electrical and computer

engineering from Georgia Institute of Technology, Atlanta, GA, USA, in 2014. He is currently a postdoctoral associate in the Department of Electrical Engineering and Computer Science, Massachusetts Institute of Technology (MIT), Cambridge, MA, USA. His research interests include analog/mixed-signal/power-management integrated circuit and system design for implantable biomedical applications. Dr. Lee received Silver Prizes in the 16th and 18th Human-Tech Thesis contest from Samsung Electronics, Korea, in 2010 and 2012, respectively, and a Commendation Award associated with the 4th Outstanding Student Research Award from TSMC, Taiwan, in 2010. He is a member of the IEEE.



**Maysam Ghovanloo** received a BSc in electrical engineering from the University of Tehran, Tehran, Iran, in 1994, an MSc in biomedical engineering from the Amirkabir University of Technology, Tehran, Iran, in 1997, and an MSc and a PhD in electrical engineering from the University of Michigan, Ann Arbor, MI, USA, in 2003 and 2004, respectively. From 2004 to 2007, he was an Assistant Professor in the Department of Electrical and Computer Engineering, North Carolina State University, Raleigh, NC, USA. He joined the faculty of the Georgia Institute of Technology, Atlanta, GA, USA, in 2007, where he is currently an Associate Professor and the Founding Director of the Georgia Tech Bionics Lab in the School of Electrical and Computer Engineering. He has authored or coauthored more than 150 conference and journal publications. Dr. Ghovanloo is an Associate Editor of *IEEE Transactions on Biomedical Circuits and Systems* and *IEEE Transactions on Biomedical Engineering*. He is the general chair of the 2015 IEEE Biomedical Circuits and Systems (BioCAS) Conference. He served on the IEEE International Solid-State Circuits Conference (ISSCC) subcommittee for imagers, MEMS, medical, and displays from 2010–2014. He received awards in the 40th and 41st DAC/ISSCC Student Design Contests. He organized special sessions and was a member of technical review committees for several major conferences, such as ISSCC and ISCAS, in the areas of biomedical circuits, sensors, and systems. He is a member of Tau Beta Pi, Sigma Xi, the IEEE Solid-State Circuits Society, the IEEE Circuits and Systems Society, and the IEEE Engineering in Medicine and Biology Society. He is a senior member of the IEEE.